Microstructure Evolution and Mechanical Behavior of a CMnSiAl TRIP Steel Subjected to Partial Austenitization Along with Quenching and Partitioning Treatment

H. KONG, Q. CHAO, M.H. CAI, E.J. PAVLINA, B. ROLFE, P.D. HODGSON, and H. BELADI

The present study investigated the microstructure evolution and mechanical behavior in a low carbon CMnSiAl transformation-induced plasticity (TRIP) steel, which was subjected to a partial austenitization at 1183 K (910 °C) followed by one-step quenching and partitioning (Q&P) treatment at different isothermal holding temperatures of [533 K to 593 K (260 °C to 320 °C)]. This thermal treatment led to the formation of a multi-phase microstructure consisting of ferrite, tempered martensite, bainitic ferrite, fresh martensite, and retained austenite, offering a superior work-hardening behavior compared with the dual-phase microstructure (*i.e.*, ferrite and martensite) formed after partial austenitization followed by water quenching. The carbon enrichment in retained austenite was related to not only the carbon partitioning during the isothermal holding process, but also the carbon enrichment during the partial austenitization and rapid cooling processes, which has broadened our knowledge of carbon partitioning mechanism in conventional Q&P process.

I. INTRODUCTION

THE requirements of vehicle weight reduction and improved crash performance have promoted the development of new generations of advanced high strength steels (AHSS) with a good combination of strength and ductility. As one of the promising path towards these properties, quenching and partitioning (Q&P) heat treatment[1,2] has attracted considerable interest in the last several years. This treatment aims to retain some austenite at room temperature that will transform into martensite upon straining, delaying the onset of necking through the transformation-induced plasticity (TRIP) effect,[3] which ultimately offers excellent work-hardening behavior.

The concept of the Q&P process is to develop a multi-phase microstructure in steels, mainly consisting of martensite, retained austenite, and/or ferrite.[1,2,4,5] In a typical Q&P process, the steel is initially subjected to a full or partial austenitization treatment, which is followed by rapid cooling to a temperature between the martensitic transformation starting temperature (M_s) and finishing temperature (M_f) to form a certain fraction of martensite. The steel is subsequently held either at the same temperature (*i.e.*, a one-step Q&P process) or at a higher temperature (*i.e.*, a two-step Q&P process) to allow carbon partitioning from the initial supersaturated martensite to the untransformed austenite. Finally, the steel is quenched to room temperature, where the austenite with insufficient carbon enrichment is likely to transform into fresh martensite while the sufficiently stabilized austenite may be retained at ambient temperature.

The extent of the carbon enrichment in retained austenite is dependent on the steel composition and heat treatment schedules. Most of the current research has been focused on the Q&P processing of low carbon steels after full austenitization, which normally produces a duplex microstructure composed of martensite and retained austenite.[6–10] Here, the carbon enrichment in the retained austenite is mostly ascribed to the carbon rejection from the initial supersaturated martensite. In comparison, if the Q&P processing is performed

H. KONG, Q. CHAO, P.D. HODGSON, and H. BELADI are with the Institute for Frontier Materials, Deakin University, Geelong, VIC 3216, Australia. Contact e-mail: hossein.beladi@deakin.edu.au M.H. CAI is with the School of Materials Science and Engineering, Northeastern University, Shenyang 110819, China. E.J. PAVLINA is with the AK Steel Research and Innovation Center, Middletown, OH 45005. B. ROLFE is with the Institute for Frontier Materials, Deakin University and also with the School of Engineering, Deakin University, Geelong, VIC 3216, Australia.

following partial austenitization, one can expect higher extent of carbon and manganese diffusion from ferrite into the intercritical austenite due to the different solubilities in these two phases, which would further stabilize the austenite.[11] Moreover, proeutectoid ferrite might form upon the initial cooling from the partial austenitization treatment temperature, further contributing to the partition of carbon into neighboring austenite.[11–13] During the subsequent isothermal holding process, the remaining austenite would be further stabilized through the carbon partitioning from the preformed martensite. However, more recently, bainitic transformation may take place during the isothermal process at a temperature either above or below the M_s temperature,[12,14–22] and this could further stabilize the remaining austenite by rejecting carbon into adjacent austenite, even though the formation of bainite may reduce the fraction of unstable austenite.[17,23,24] The phase transformation behavior would be more interesting if the steel is partitioned below M_s temperature or undergo the one-step Q&P processing, which has recently attracted much attention. However, there is limited research[12] on the isothermal phase transformation behavior during holding below the M_s temperature with the presence of pre-existing ferrite if partial austenitization is applied. This thermal treatment may result in a complicated mechanism of carbon enrichment in retained austenite and the formation of its final morphologies, which will be a point of interest to be investigated in the current study.

In the present study, one-step Q&P processing following prior partial austenitization was performed in a C-Mn-Si-Al TRIP steel. The aim is to systemically examine the influences of intercritical annealing, rapid cooling, and isothermal holding processes on the microstructure evolution and the resultant mechanical behaviors. In particular, the microstructure evolution and mechanical performance during the Q&P process at different isothermal holding temperatures [533 K to 593 K, (260 °C to 320 °C)] were examined in comparison with a direct water-quenched condition.

II. EXPERIMENTAL PROCEDURE

A. Material

The material used in the current study was cold-rolled TRIP steel sheet with a thickness of ~ 2.0 mm supplied by Wuhan Iron Steel Corp. (WISCO), China. The chemical composition is shown in Table I. The as-received microstructure consisted of ~ 53 pct ferrite along with ~ 35 pct bainite, and ~ 12 pct retained austenite (Figure 1(a)). The critical austenite start and finish temperatures (A_{c1} and A_{c3}) on reheating at a rate of 30 K/s and martensite start and finish temperatures (M_s and M_f) on cooling at a rate of 80 K/s were determined to be [1039 K, 1273 K, 496 K, and 668 K (766 °C, 1000 °C, 223 °C, and 395 °C)], respectively (Figure 1(b)) using a DIL805 dilatometer (TA Instruments, Germany). Here, rectangular flat specimens with

Table I. Chemical Composition of the Current TRIP Steel, in Weight Percent

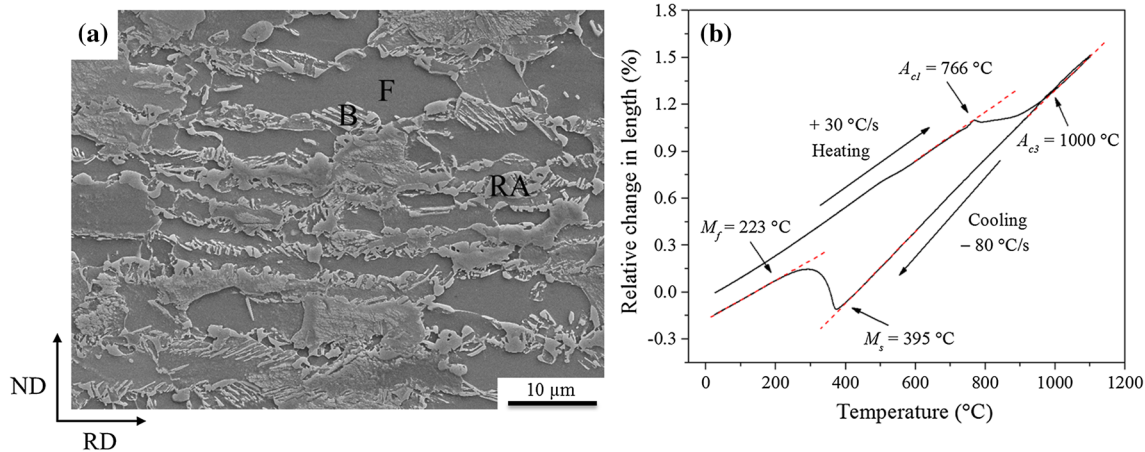|	C	Mn	Si	Al	Fe
Melt composition	0.25	1.45	0.52	1.13	balance
Estimated austenite composition at 1183 K (910 °C) using Thermo-Calc software	0.31	1.62	0.52	0.95	balance

Fig. 1—(a) SEM micrograph of the as-received TRIP steel. F, B, and RA correspond to ferrite, bainite, and retained austenite, respectively. (b) Dilatometric curve of the experimental TRIP steel during the reheating and cooling processes. A_{c1}, A_{c3}, M_s, and M_f are the starting and finishing temperatures for the formation of austenite and martensite, respectively. RD and ND represent rolling direction and normal direction, respectively.

the dimension of 10 mm × 4 mm × 2 mm were used for the dilatometry testing. Compressed nitrogen gas was used as the cooling medium.

B. One-step Quenching and Partitioning Treatment

The as-received TRIP steel sheet was subjected to different heat treatments (Figure 2). During the one-step Q&P treatment, the specimens were reheated in a fluidized bed furnace under an argon atmosphere to 1183 K (910 °C) at a rate of approximately 30 K/s and held for 5 minutes to partially transform the initial microstructure to austenite. The steels were subsequently transferred to a salt bath furnace set at different isothermal temperatures of [533 K, 563 K, and 593 K (260 °C, 290 °C, and 320 °C)] for 90 seconds, followed by water quenching to room temperature. The cooling rate in the salt bath furnace was estimated to be ~ 80 K/s. Another sample was directly water-quenched from 1183 K (910 °C) after the partial austenitization treatment to produce a dual-phase microstructure. The specimen temperature was measured by a thermocouple inserted into a hole drilled in the specimen. Similar heat treatment cycles to the Q&P heat treatments were simulated using the dilatometer in the current work to study the phase transformation behavior of the steel.

C. Microstructure Characterization

Microstructural characterization of the heat-treated steels was performed on the normal direction–rolling direction (ND–RD) plane, using scanning electron microscopy (SEM) including electron backscatter diffraction (EBSD). A standard mechanical polishing including a finishing polish routine with a 0.04 μm colloidal silica suspension (OPS, Struers, Denmark) was employed for preparing samples for SEM analysis. A final 2 vol pct nital etching was carried out where applicable. SEM imaging was performed using a field emission gun (FEG) SEM (Zeiss-Supra 55VP, Germany) integrated with an angle-selective backscattered (AsB) detector.[25] EBSD analysis was carried out using Zeiss Leo 1530 FEG-SEM equipped with a fully automatic *Aztec HKL* EBSD attachment (Oxford Instrument, UK), operated at 20 kV and a step size of 50 nm. The *HKL* Channel 5 software was used for post processing of the EBSD data.

X-ray diffraction (XRD) analysis was implemented for phase identification on the rolling direction–transverse direction (RD–TD) plane of the current steel treated under different conditions before and after tensile testing, using PANalytical X'Pert PRO MRD (XL) X-ray diffractometer with Cu K$_\alpha$ radiation, operated at 40 kV and 30 mA. After fracture, XRD measurements were performed at a location close to the fracture surface in the gauge area. The XRD specimens were prepared following a standard practice composed of successive grinding, mechanical polishing, and chemical thinning as described in the ASTM Specification E975-13.[26] The final chemical thinning was conducted using a solution of an equal volume ratio of nitric acid, hydrochloric acid, and distilled water.[27] This corrosive
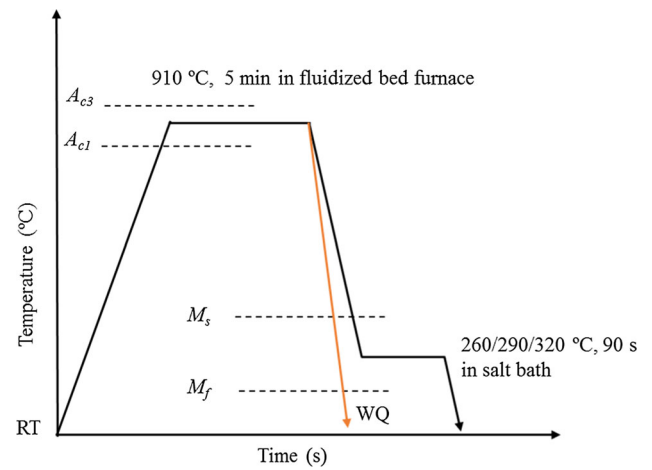

Fig. 2—Schematic representation of the direct water-quenching and one-step Q&P treatments of the TRIP steel. RT and WQ indicate room temperature and water-quenching, respectively. A_{c1}, A_{c3}, M_s, and M_f are the starting and finishing temperatures for the formation of austenite and martensite, respectively.

solution removed ~ 250 μm of the surface layer, where the retained austenite may have transformed to martensite during sample preparation. The fraction of retained austenite was calculated using a direct comparison method with the integrated intensities of (111)γ, (200)γ, (220)γ, and (311)γ peaks, and (110)α, (200)α, and (211)α peaks.[26] The austenite lattice parameter, a_γ, was determined by the positions of the four austenite peaks using Cohen's method.[28] The carbon content in the retained austenite was estimated by the following equation[29]:

$$\alpha_\gamma = 0.3556 + 0.00453x_C + 0.000095x_{M_n} + 0.00056x_{Al},$$

[1]

where a_γ is the austenite lattice parameter in nm and x_C, x_{M_n}, and x_{Al} are the concentrations of carbon, manganese, and aluminum in austenite, respectively (in wt pct). Note that x_{M_n} and x_{Al} represent the equilibrium values in austenite at 1183 K (910 °C) calculated by the Thermo-Calc software (see Table I). The effect of silicon was not considered in Eq. [1]. The carbon content in austenite represents the average value for all austenite grains despite the possible variation of carbon content in austenite grains of different morphologies (block or film) or a single austenite grain (carbon gradient) due to the insufficient partitioning process during partial austenitization, subsequent cooling, and isothermal holding processes.

D. Tensile Testing

The tensile specimens were machined from the heat-treated sheets having 25 mm gauge length and 5 mm gauge width. Uniaxial tensile testing was performed using Instron 30 kN 5967 machine equipped with a non-contact extensometer at a true strain rate of 1.0×10^{-3} s^{-1}. The work-hardening behavior was analyzed using Hollomon's equation[30]:

$$\sigma = K\varepsilon^n, \qquad [2]$$

where σ and ε are true stress and true strain, respectively, K is a constant, and n is the instantaneous work-hardening exponent and could be calculated using the following equation:

$$n = \frac{\varepsilon d\sigma}{\sigma d\varepsilon} \qquad [3]$$

The criterion for necking is: $\frac{d\sigma}{d\varepsilon} = \sigma$, thus $n = \varepsilon_\mu$, where ε_μ is the uniform elongation.

III. RESULTS AND DISCUSSION

A. Microstructure Evolution

1. Partial austenitization

In the current study, the microstructure evolution throughout the heat treatment was extensively investigated by dilatometry followed by microstructure characterization. The volume fraction of austenite after partial austenitization was estimated to be ~ 78 pct using the lever rule along with the dilatation curve of the fully austenitized specimen (Figure 1b). This resulted in a change in the composition of the remaining austenite at 1183 K (910 °C), enriching the carbon content to an average value of ~0.31 wt pct based on the Thermo-Calc calculation (Table I). In addition, this treatment might cause a heterogeneous carbon concentration in different austenite grains after reheating the as-received multi-phase microstructure at 1183 K (910 °C) (Figure 1a). For example, austenite grains that form in the vicinity of cementite typically contain a higher carbon content than other regions. This variation in carbon concentration could lead to diverse phase transformation behaviors in the remaining austenite on cooling.
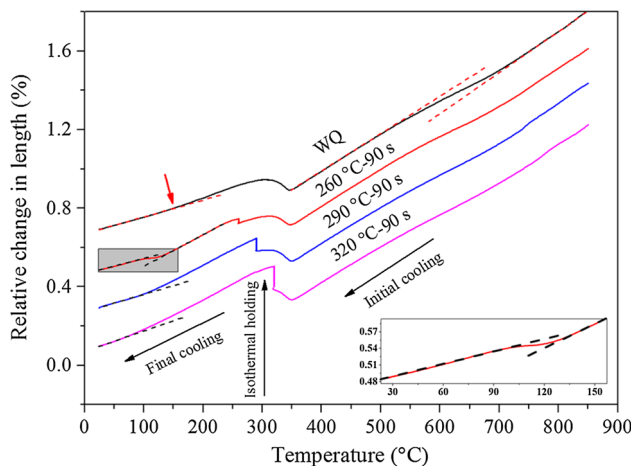

Fig. 3—Relative change in length as a function of temperature for different dilatometry schedules. The gray square is enlarged in the right bottom, showing the fresh martensite formation upon final cooling after the completion of isothermal holding treatment.

2. Initial rapid cooling

When the steel was subjected to the first rapid cooling process after partial austenitization, there was a length dilatation at a temperature range of [~ 1036 K to ~ 775 K (~ 763 °C to ~ 502 °C)] for all heat treatment schedules (Figure 3), suggesting that the results are consistent and reproducible. This dilation might be related to the proeutectoid ferrite transformation upon rapid cooling.[12] This transformation is consistent with the shadow-like (i.e., image contrast difference) regions appearing in the ferrite grains. They were mostly in the vicinity of the second phase (Figures 4(b), (d), (f), and (h)), which confirms the formation of proeutectoid ferrite for both Q&P processed and direct water-quenched conditions. Similar observations have been reported by others[12] and the shadow-like region in ferrite was referred to as epitaxial ferrite. The untransformed ferrite and newly formed epitaxial ferrite were mostly elongated along the rolling direction (Figure 4), with a volume fraction of 26 ± 1.4 pct and an average grain size of 2.6 ± 0.1 μm. Noticeably, the total volume fraction of ferrite obtained after the completion of the heat treatment schedule was slightly higher than that estimated from dilatometry experiments (i.e., ~ 22 pct), most likely ascribed to the formation of epitaxial ferrite.

Further cooling revealed a dramatic volume expansion at a temperature of ~ 624 K (~ 351 °C) for all heat treatment conditions, indicating the occurrence of a martensitic transformation. As a result, the ferrite grains adjacent to the martensite may have been deformed, exhibiting dislocations in the grain interiors (Figure 5).[31] This temperature can be referred to as the martensitic transformation starting temperature of the partially transformed austenite (hereafter referred to as M'_s), which is significantly lower than the full austenitization condition due to the aforementioned carbon enrichment in austenite during partial austenitization and subsequent epitaxial ferrite formation. Below the M'_s temperature, the dilatation curve behavior changed depending on the heat treatment conditions, representative of different phase transformation behavior that occurred afterwards. As for the continuous cooled sample, representing the water-quenched condition after the partial austenitization treatment, the dilatation increased continuously up to a temperature of ~ 573 K (~ 300 °C), beyond which there was a linear contraction with a decrease in the temperature (i.e., negative dilatation slope). Another slight slope change also appeared at ~ 426 K (~ 153 °C) (shown by red arrow in Figure 3), which is most likely related to the continuous formation of martensite from the remaining austenite with higher carbon content. As mentioned previously, some of the austenite has been enriched in carbon during the partial austenitization and subsequent cooling sequences. In addition, the level of carbon content is expected to be non-uniform and to depend on the size of the austenite island and where it was formed. As a result, the M'_s temperature may locally vary and each region of austenite will transform over a different temperature range on cooling. However, it appeared that such level of carbon enrichment might be
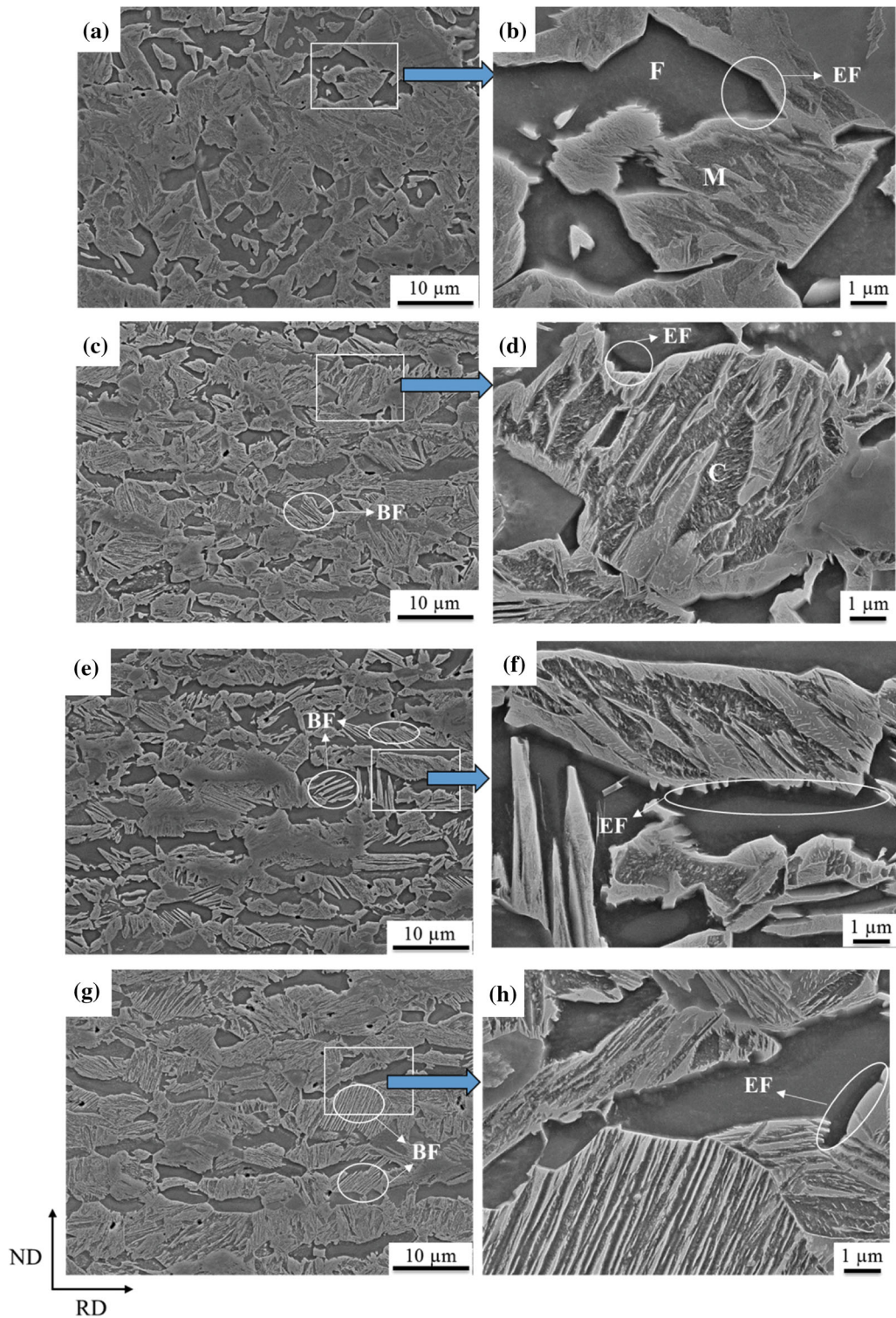
Fig. 4—SEM micrographs of the (*a*, *b*) water-quenched and one-step Q&P processed TRIP steels at isothermal holding temperatures of (*c*, *d*) 533 K (260 °C), (*e*, *f*) 563 K (290 °C), and (*g*, *h*) 593 K (320 °C). The white squares in the left images (a, c, e, and g) are enlarged in the right images (b, d, f, and h). F, M, C, BF, and EF indicate ferrite, martensite, carbides, bainitic ferrite, and epitaxial ferrite, respectively. RD and ND represent rolling direction and normal direction, respectively.

insufficient for the austenite to be retained at room temperature. As shown in Figure 6(a), no austenite peaks appeared in the XRD spectra, suggesting that the austenite has most likely transformed fully into martensite during the water-quenching process. As a consequence, a dual-phase microstructure consisting of martensite and ferrite was mainly formed in the direct water-quenched steel.
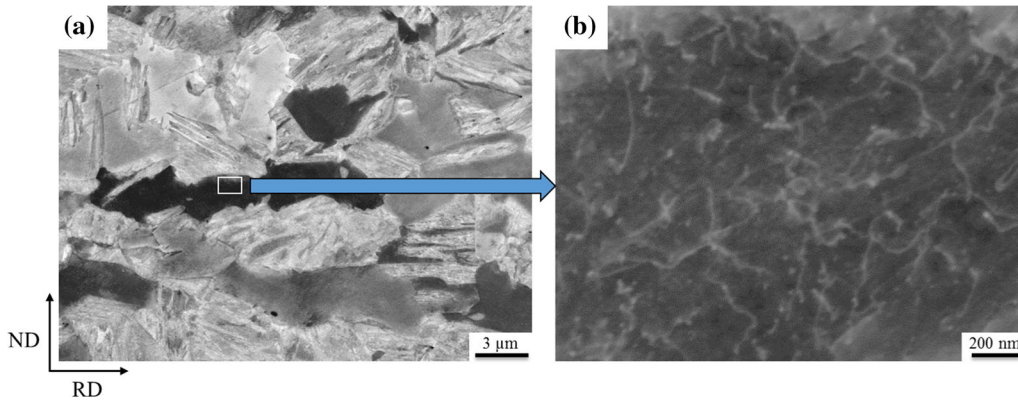
Fig. 5—SEM-AsB micrographs of the current TRIP steel isothermally held at 563 K (290 °C) for 90 s. The white square in image (*a*) is enlarged in image (*b*) showing the dislocations in ferrite. RD and ND represent rolling direction and normal direction, respectively.
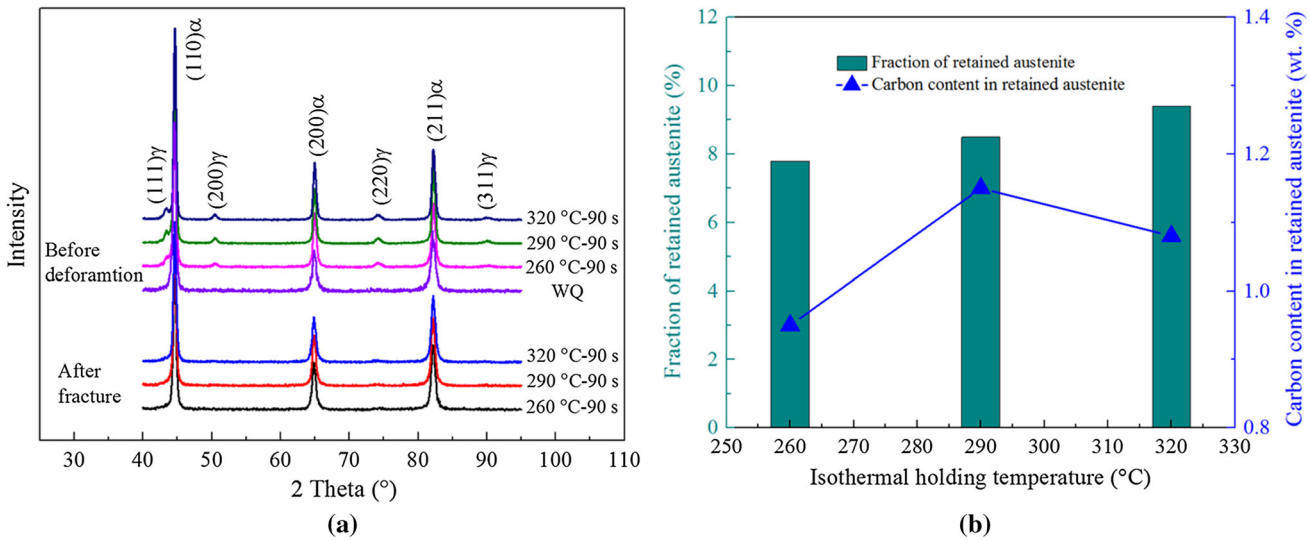

Fig. 6—(*a*) XRD spectra of the TRIP steel subjected to different heat treatment schedules before and after tensile testing. (*b*) The calculated retained austenite fraction and carbon content of the Q&P processed steels under different conditions.

3. Isothermal holding

For the Q&P processed conditions, austenite partially transformed to martensite when the steel was rapidly cooled to the isothermal temperature. The fraction of martensite progressively increased with a decrease in the isothermal temperature, from ~ 21 pct at 593 K (320 °C) to ~ 36 pct at 563 K (290 °C), and ~ 47 pct at 533 K (260 °C) calculated from the dilation curves using the Koistinen and Marburger (K–M) model.[32] Accordingly, the fraction of remaining austenite is estimated, ~ 53 pct at 593 K (320 °C), ~ 38 pct at 563 K (290 °C), and ~ 27 pct at 533 K (260 °C). Significant dilatations were observed below the M'_s temperature in all specimens during isothermal holding (Figure 3). The extent of dilatation though altered depending on the isothermal holding temperature, the dilatation increased with the isothermal temperature from 0.032 to 0.065 pct, and 0.113 pct for [533 K, 563 K, and 593 K (260 °C, 290 °C, and 320 °C)], respectively. This is mainly associated with the

formation of bainitic ferrite during the holding process.[14–16,19,22] As the isothermal temperature was reached, the martensite supersaturated in carbon is tempered and rejects carbon into adjacent remaining austenite (*i.e.*, carbon partitioning).[1,33] It has been reported by the current authors[34] that the partitioning time of 90 seconds might be inadequate for the completion of the carbon homogenization in austenite at the current isothermal holding temperatures, particularly for blocky/coarse austenite grains/islands (Figures 7(b) and (d)). Thus, a steep carbon gradient within a single austenite grain is expected in the present study, which has also been reported by others.[11,35–38] Additionally, the aforementioned carbon enrichment in the remaining austenite, resulting from both the partial austenitization treatment and the epitaxial ferrite formation, significantly contributes to the heterogeneity of the carbon concentration in the austenite. This heterogeneity suggests that, in the current study, the remaining austenite before isothermal holding most likely appears in both
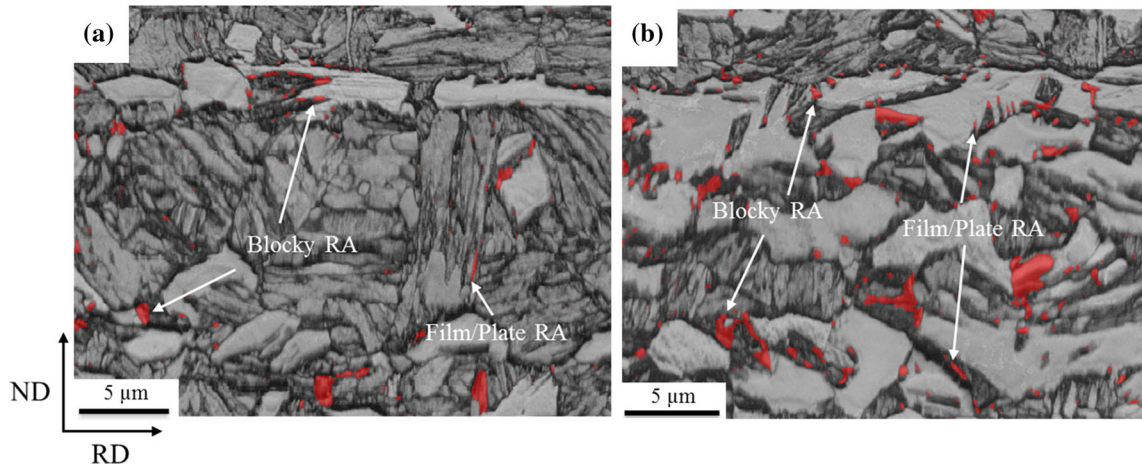
Fig. 7—EBSD band contrast combined with color-coded phase maps of the one-step Q&P processed steels at different isothermal temperatures of (a) 533 K (260 °C) and (b) 563 K (290 °C), where red areas represent fcc structures. RD and ND represent rolling direction and normal direction, respectively.
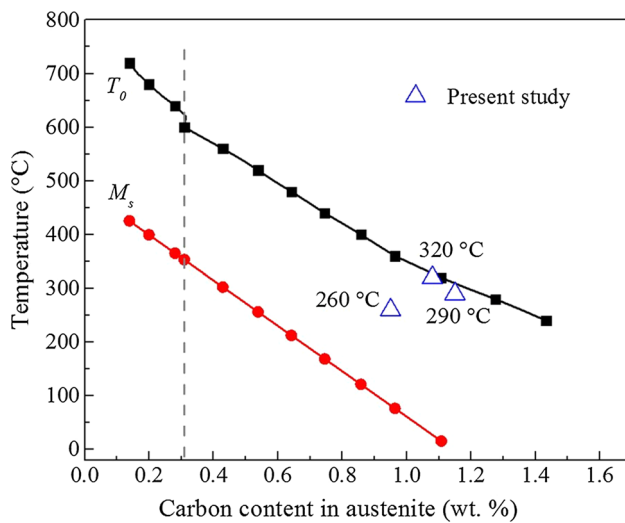

Fig. 8—Calculated T_o and M_s temperature of the present steel as a function of carbon content in austenite. The dashed line represents the overall carbon content in steel at 1183 K (910 °C). The three open triangle symbols indicate the measured carbon content in retained austenite at room temperature under different isothermal holding temperatures (i.e., 533 K (260 °C), 563 K (290 °C), and 593 K (320 °C)).

low carbon and carbon-rich regions. Therefore, the martensitic and bainitic start transformation temperatures (M_s and B_s) of the carbon-rich austenite would be relatively lower than that of the low carbon austenite. As the carbon partitioning proceeds, the M_s temperature of the carbon-rich austenite would be further decreased and becomes lower than the isothermal holding temperature. As a result, this austenite is expected to transform into bainite as the holding time increases and simultaneously further rejects carbon to neighboring austenite.[24]

The second phase islands that were formed during Q&P treatments appeared differently compared with the direct water-quenched condition (i.e., martensitic island) after etching by nital. SEM characterization of these

regions exhibited martensitic characteristics containing carbides (i.e., transition carbide formation), whereas the other region showed lamellar structure. These microstructure characteristics were frequently observed under all Q&P conditions, particularly at higher isothermal temperatures (for example, 593 K (320 °C), Figures 4(c) through (h)). The lamellar structure in SEM and EBSD micrographs (Figures 4(c) through (h) and 7(a) and (b)) most likely represents bainitic ferrite.

The decomposition of austenite into bainite during the isothermal holding process, particularly at a temperature below M_s, has recently attracted a lot of attention.[12,15,16,19–21,39,40] A small amount of pre-formed athermal martensite is considered to be able to markedly accelerate the bainitic transformation kinetics by providing more nucleation sites,[15,19,21,22,39] compared with those where the steel is cooled to a temperature with a high undercooling below M_s.[41,42] To further clarify the formation kinetics of bainitic ferrite in the present study, the incubation time for the bainite formation is calculated using the method developed by Bhadeshia[43] and also used elsewhere.[12,44,45] The bainitic incubation time was estimated to be 60 seconds at 593 K (320 °C), 180 seconds at 563 K (290 °C), and 705 seconds at 533 K (260 °C). Thus, the isothermal holding time of 90 seconds is sufficient for the bainite formation at 593 K (320 °C), but might be insufficient at [563 K and 533 K (290 °C and 260 °C)]. However, it might be still possible for the current steel to form bainite under these two conditions considering the aforementioned accelerated effect by the presence of a small amount of martensite.[19,21] As a result, in the present study, the bainite is most likely to form when the steel is isothermally held for a certain time at a temperature below M'_s. This phenomenon is more pronounced when a small undercooling below M'_s is applied, for example, the 593 K (320 °C) condition for the current steel. The bainitic transformation ceases when the carbon content in austenite reaches the T_o curve, (Figure 8, T_o is a temperature at which free energies of austenite and bainitic ferrite having the same
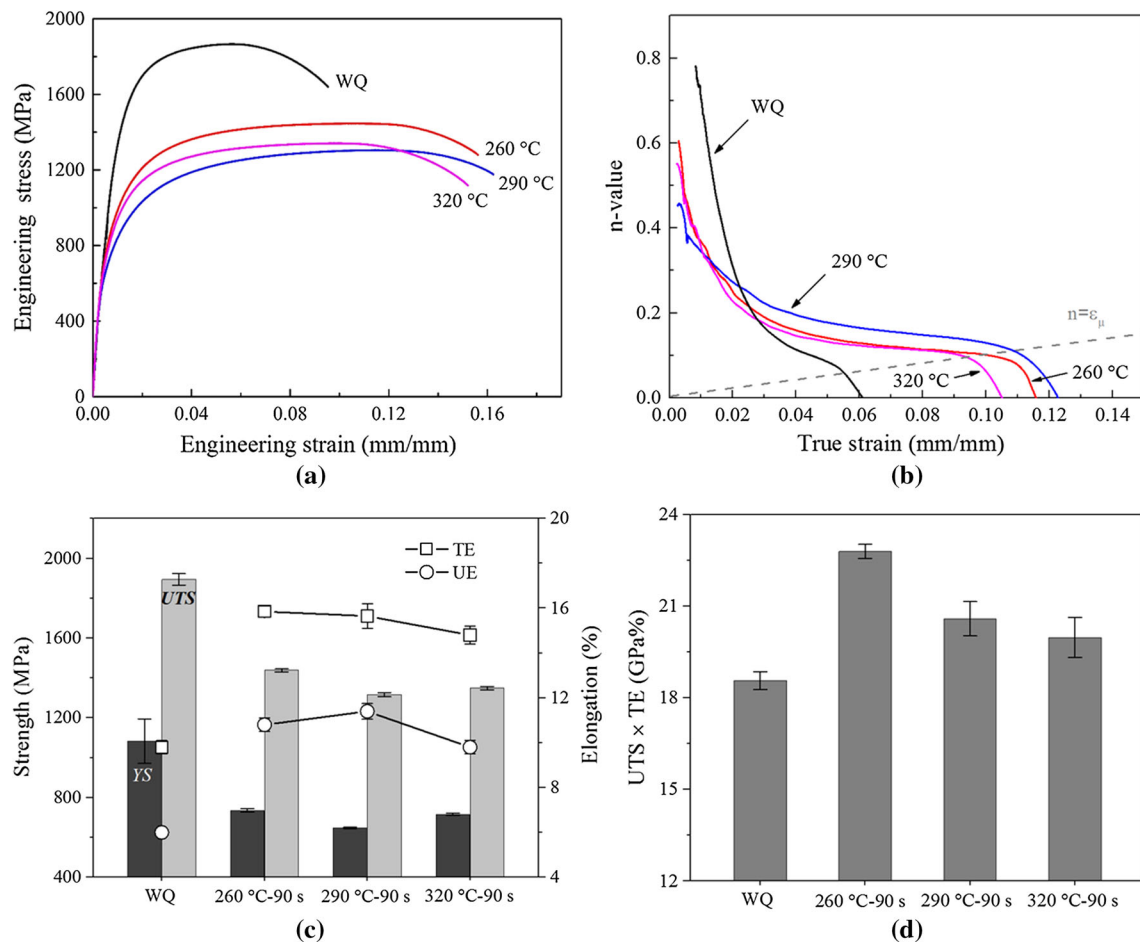
Fig. 9—(*a*) Engineering stress–engineering strain curves, (*b*) instantaneous work-hardening (*n*-value) curves, (*c*) tensile properties, and (*d*) formability index for the water-quenched and one-step Q&P processed TRIP steels. YS, UTS, UE, and TE indicate yield strength, ultimate tensile strength, uniform elongation, and total elongation, respectively.

composition are equal),[46] which is called the incomplete reaction phenomenon.[47] The T_o value of the present steel is calculated using the method proposed by *Peet* and *Bhadeshia*[45] (Figure 8). The experimental carbon content in the retained austenite measured by XRD is approaching the T_o curve, particularly for samples isothermally held at [593 K and 563 K (320 °C and 290 °C)]. This correspondence suggests the occurrence of a bainitic phase transformation and the rejection of carbon into adjacent austenite at these isothermal temperatures.

4. *Final cooling*

During further cooling after the isothermal holding process, there was a linear contraction observed for all Q&P conditions. Similar to the continuous cooled sample, a slight slope change was observed at the temperature of [~ 405 K, ~ 375 K, and ~ 353 K (~ 132 °C, ~ 102 °C, and ~ 80 °C)] for the isothermal holding temperatures of [533 K, 563 K, and 593 K (260 °C, 290 °C, and 320 °C)], respectively. This slope change may be due to the formation of fresh martensite from remaining austenite with insufficient carbon

enrichment, which was more significant under the 533 K (260 °C) condition compared to the other two Q&P conditions (Figure 3).

Apart from the fresh martensite formation from the remaining low carbon austenite, some other austenite with adequate carbon enrichment was retained at room temperature (Figures 6 and 7). The fraction of retained austenite increased gradually with the isothermal holding temperature, from 7.8 ± 0.2 pct at 533 K (260 °C) to 9.4 ± 0.3 pct at 593 K (320 °C) (Figure 6(b)). The carbon content in the retained austenite was calculated to be ~ 0.95 wt pct at the isothermal holding temperature of 533 K (260 °C) and further increased to ~ 1.15 wt pct at 563 K (290 °C), and then reduced to ~ 1.08 wt pct at 593 K (320 °C) (Figure 6(b)). The retention of austenite is most likely associated with further carbon partitioning during the isothermal holding process besides the initial carbon enrichment from the partial austenitization and epitaxial ferrite formation as no austenite was retained for the direct water-quenched condition. The increase in the retained austenite fraction with the isothermal temperature agreed well with the increase in the austenite fraction

remaining for partitioning at the beginning of the isothermal holding process. The enhanced partitioning kinetics as well as the remarkable formation of bainitic ferrite at high temperatures (for example, 593 K (320 °C)) might also account for the corresponding increase in the retained austenite fraction. However, the lower fraction of preformed martensite at 593 K (320 °C) is most likely responsible for the lower carbon content in the retained austenite (~ 1.08 wt pct), compared to the 563 K (290 °C) condition (~ 1.15 wt pct), because of the reduced amount of carbon for partitioning.

In addition, the retained austenite was observed in two types of morphologies in the microstructure through the EBSD examination: blocky retained austenite; mostly distributed in the vicinity of the ferrite grains and film/plate retained austenite; commonly observed as films/plates between martensite or bainitic ferrite laths (Figure 7). Not all film-like retained austenite was indexed by EBSD due to its small thickness, typically in the range of 20 to 100 nm,[15,48–50] which is mostly lower than the spatial resolution of the EBSD technique (i.e., 50 nm, which was used in the current study). The mechanism of the carbon enrichment in retained austenite differs, depending on its morphology. For the blocky retained austenite located in the ferrite grain boundaries, it might be firstly enriched in carbon during the partial austenitization and the formation of epitaxial ferrite, and further stabilized by the carbon partitioning during the isothermal holding process. For the film-like retained austenite between martensite or bainitic ferrite laths, it is most likely ascribed to the carbon partitioning from martensite and isothermally formed bainitic ferrite upon isothermal holding.

In general, in the current heat treatment schedules, a dual-phase microstructure composed of martensite and ferrite was produced in the direct water-quenched condition. However, a multi-phase microstructure consisting of ferrite, tempered martensite, bainitic ferrite, fresh martensite, and retained austenite was exhibited in the Q&P processed condition. The retention of austenite is attributed to the combined effects of carbon enrichment from the partial austenitization, epitaxial ferrite formation, and the carbon partitioning from martensite and isothermally formed bainitic ferrite.

B. *Mechanical Behavior*

The current microstructures that were obtained in the Q&P processed steel offered a superior work-hardening performance in comparison with the direct water-quenched condition (Figures 9(a) and (b)). For the direct water-quenched steel, a high instantaneous work-hardening exponent (i.e., n-value) was observed at the beginning of straining and it then declined remarkably. Soft ferrite phases deform initially, but the deformation ability of ferrite is limited,[51] resulting in straining of the martensite during further deformation. The high n-value at the beginning of deformation is likely due to the high fraction of martensite (i.e., 74 pct experimentally) containing high density of dislocations.[10,51,52] However, the interaction of dislocations

could contribute to a significant decrease in n-value during the late stage of straining.[53] This thermal treatment ultimately resulted in a yield strength (YS) of 1083 ± 112 MPa and a high ultimate tensile strength (UTS) of 1894 ± 29 MPa along with the uniform and total elongations (i.e., UE and TE) of 6.0 ± 0.3 and 9.8 ± 0.3 pct, respectively (Figure 9(c)).

For the Q&P processed steels, the work-hardening behavior could be divided into three stages based on the difference in the slope of the instantaneous work-hardening curves (Figure 9(b)). At the first stage of straining, the n-value was high at the beginning and then decreased continuously. The comparatively lower n-value is associated with the presence of retained austenite and the lower fraction of martensite compared with the direct water-quenched steel. Also, the unpinned dislocations in ferrite (Figure 5) should be considered responsible for a decrease in the n-value.[31] In addition, a lower dislocation density in martensite resulting from the tempering treatment on isothermal holding gives rise to the increased deformation capability of martensite.[10] Therefore, the Q&P processed steels revealed much lower yield strength than that of the water-quenched steel, which also depended on the isothermal holding temperature. The YS decreased from 736 ± 9 to 647 ± 4 MPa as the isothermal temperature increased from [533 K to 563 K (260 °C to 290 °C)]. Afterwards, it increased to 716 ± 6 MPa at the isothermal temperature of 593 K (320 °C). It should be noted that the n-value of the steel isothermally held at 563 K (290 °C) was initially lower and then became higher than that of the other two conditions (i.e., [533 K and 593 K (260 °C and 320 °C)]). The higher n-values at 533 K (260 °C) and 593 K (320 °C) at the beginning may be explained by the higher fractions of tempered martensite and fresh martensite at 533 K (260 °C), and the significant presence of bainitic ferrite at 593 K (320 °C). The latter resulted in an increased carbon content in the adjacent unstable austenite (i.e., lower fresh martensite start transformation temperature upon final water quenching, Figure 3), which might further enhance the solid solution strengthening of the fresh martensite.[54] As the straining proceeds, there might be strain-induced martensitic transformation of unstable blocky austenite (Figure 7(b)) for the 563 K (290 °C) condition, which simultaneously enhances the work-hardening.

At the second stage, the work-hardening exponent decreased slowly and became nearly constant. This led to the distinct changes in total/uniform elongations, showing a slight decline in TE from 15.9 ± 0.3 to 14.8 ± 0.4 pct whereas a continuous increase followed by a slow decrease in UE from 10.8 ± 0.3 to 11.4 ± 0.4 and 9.8 ± 0.3 pct as the isothermal temperature increased from [533 K to 593 K (260 °C to 320 °C)]. In the current study, the retained austenite almost fully transformed into martensite at failure (Figure 6(a)). This transformation behavior could contribute to the work-hardening and hence delay the onset of necking, suggesting the enhancement of both strength and ductility (i.e., TRIP effect).[3] Thus, this plateau-like stage is mainly related to the TRIP effect of the retained austenite.[53] Generally, more retained austenite might give rise to a more

pronounced TRIP effect and then higher *n*-value.[55] However, the highest fraction of retained austenite was observed at 593 K (320 °C), which was not in agreement with the highest *n*-value shown at 563 K (290 °C). This disagreement may be explained by the different stabilities of austenite retained under these heat treatment conditions. In general, the retained austenite with a lower stability would transform into martensite at a lower strain. The stability of retained austenite mainly depends on: (i) chemical composition especially carbon content in austenite[56]; (ii) size and morphology[57]; (iii) surrounding phases.[58] In the present study, the highest carbon content was obtained at 563 K (290 °C), suggesting the higher stability of retained austenite at this condition. Thus, it is reasonable that the highest *n*-value is observed in the steels isothermally held at 563 K (290 °C). The morphology of retained austenite plays a significant role in its stability in a Q&P steel.[48] In the present steel, the retained austenite appears in different morphologies including blocks and films (Figures 7(a) and (b)). The broader plateau region of work-hardening might be associated with the continuous TRIP effect of the retained austenite with different stabilities. This effect ultimately resulted in the superior mechanical behavior (*i.e.*, UTS: ~ 1400 MPa; TE: ~ 16 pct) compared to the direct water-quenched condition in which no austenite was retained. At the third stage of straining, which corresponds to the post-necking elongation, there was no obvious difference for the three Q&P conditions, exhibiting a continuous decrease of *n*-value with strain.

The formability index (*i.e.*, the product of UTS and TE) of the current steel displayed a significant increase after applying the current one-step Q&P heat treatment in comparison with the directly water-quenched condition. The lowest value of 18.6 ± 0.3 GPa pct was obtained for the direct water-quenched condition. For the Q&P processed conditions, it exhibited a continuous decrease from 22.8 ± 0.2 to 20.0 ± 0.7 GPa pct with an increase in the isothermal holding temperature from [533 K to 593 K (260 °C to 320 °C)] (Figure 9(d)). Thus, the application of one-step Q&P processing along with the partial austenitization treatment resulted in an optimum combination of strength (UTS: ~ 1400 MPa) and ductility (TE: ~ 16 pct) at the 533 K (260 °C) condition.

IV. CONCLUSIONS

In the current study, one-step Q&P processing combined with partial austenitization treatment was applied to a CMnSiAl TRIP steel. The phase transformation behavior during the intercritical annealing, subsequent cooling, isothermal holding, and final cooling processes was investigated. In addition, the effect of the multi-phase microstructure on the work-hardening behavior was also discussed. The following conclusions were drawn:

(i).   The present one-step Q&P processing with prior partial austenitization treatment resulted in a multi-phase microstructure composed of pre-existing and epitaxial ferrite, tempered martensite, bainitic ferrite, fresh martensite, and retained austenite, which were formed in a complex phase transformation system during the first cooling, isothermal holding, and final water-quenching processes.

(ii).   Significant amount of retained austenite was produced in the steel after the Q&P treatment, which was obtained through the redistribution of carbon during different stages of the heat treatment procedures. These include an initial carbon rejection from the pre-existing ferrite during partial austenitization and the epitaxial ferrite during rapid cooling, and also carbon partitioning from the initially formed athermal martensite and the newly formed bainitic ferrite during isothermal holding. The carbon concentration was found heterogeneous in the austenite, which brought new insights to the carbon enrichment mechanism in the one-step Q&P treatment.

(iii).   The one-step Q&P processed steels exhibited lower tensile strength but better ductility compared with the direct water-quenched ferrite + martensite dual-phase steel. A continuous decline in work-hardening with true strain was observed in the dual-phase microstructure, whereas the one-step Q&P processed steels exhibited a three-stage work-hardening behavior consisting of a broad plateau-like stage, mostly attributed to the remarkable TRIP effect of the retained austenite upon straining. This also ultimately led to an enhanced formability index of the Q&P treated samples (~ 23 GPa pct).

REFERENCES

1. J.G. Speer, D.K. Matlock, B.C. De Cooman, and J.G. Schroth: *Acta Mater.*, 2003, vol. 51, pp. 2611–22.
2. J.G. Speer, A.M. Streicher, D.K. Matlock, F. Rizzo, and G. Krauss: *Austenite Formation and Decomposition*, TMS/ISS, Warrendale, PA, 2003, pp. 505–22.
3. V.F. Zackay, E.R. Parker, D. Fahr, and R. Busch: *Trans. Am. Soc. Met.*, 1967, vol. 60, pp. 252–59.
4. D.V. Edmonds, K. He, F.C. Rizzo, B.C. De Cooman, D.K. Matlock, and J.G. Speer: *Mater. Sci. Eng. A*, 2006, vol. 438, pp. 25–34.
5. A.J. Clarke: Ph.D. Thesis, Colorado School of Mines, Golden, CO, 2006.
6. C.Y. Wang, J. Shi, W.Q. Cao, and H. Dong: *Mater. Sci. Eng. A*, 2010, vol. 527, pp. 3442–49.

7. M.J. Santofimia, L. Zhao, R. Petrov, C. Kwakernaak, W.G. Sloof, and J. Sietsma: *Acta Mater.*, 2011, vol. 59, pp. 6059–68.
8. N. Zhong, X. Wang, Y. Rong, and L. Wang: *J. Mater. Sci. Technol.*, 2006, vol. 22, pp. 751–54.
9. D. De Knijf, R. Petrov, C. Föjer, and L.A.I. Kestens: *Mater. Sci. Eng. A*, 2014, vol. 615, pp. 107–15.
10. X. Tan, Y. Xu, X. Yang, and D. Wu: *Mater. Sci. Eng. A*, 2014, vol. 589, pp. 101–11.
11. M.J. Santofimia, C. Kwakernaak, W.G. Sloof, L. Zhao, and J. Sietsma: *Mater. Charact.*, 2010, vol. 61, pp. 937–42.
12. M.J. Santofimia, L. Zhao, and J. Sietsma: *Metall. Mater. Trans. A*, 2009, vol. 40A, pp. 46–57.
13. M.J. Santofimia, L. Zhao, R. Petrov, and J. Sietsma: *Mater. Charact.*, 2008, vol. 59, pp. 1758–64.
14. S.M.C. Van Bohemen, M.J. Santofimia, and J. Sietsma: *Scripta Mater.*, 2008, vol. 58, pp. 488–91.
15. M.J. Santofimia, T. Nguyen-Minh, L. Zhao, R. Petrov, I. Sabirov, and J. Sietsma: *Mater. Sci. Eng. A*, 2010, vol. 527, pp. 6429–39.
16. P. Kolmskog, A. Borgenstam, M. Hillert, P. Hedström, S.S. Babu, H. Terasaki, and Y.-I. Komizo: *Metall. Mater. Trans. A*, 2012, vol. 43A, pp. 4984–88.
17. S. Samanta, S. Das, D. Chakrabarti, I. Samajdar, S.B. Singh, and A. Haldar: *Metall. Mater. Trans. A*, 2013, vol. 44A, pp. 5653–64.
18. E.P. Da Silva, W. Xu, C. Föjer, Y. Houbaert, J. Sietsma, and R.H. Petrov: *Mater. Charact.*, 2014, vol. 95, pp. 85–93.
19. E. Da Silva, D. De Knijf, W. Xu, C. Föjer, Y. Houbaert, J. Sietsma, and R. Petrov: *Mater. Sci. Technol.*, 2015, vol. 31, pp. 808–16.
20. M.C. Somani, D.A. Porter, L.P. Karjalainen, and R.D.K. Misra: *Metall. Mater. Trans. A*, 2014, vol. 45A, pp. 1247–57.
21. A. Navarro-López, J. Sietsma, and M.J. Santofimia: *Metall. Mater. Trans. A*, 2016, vol. 47A, pp. 1028–39.
22. S. Samanta, P. Biswas, S. Giri, S.B. Singh, and S. Kundu: *Acta Mater.*, 2016, vol. 105, pp. 390–403.
23. H. Beladi, I.B. Timokhina, X.-Y. Xiong, and P.D. Hodgson: *Acta Mater.*, 2013, vol. 61, pp. 7240–50.
24. I.B. Timokhina, K.D. Liss, D. Raabe, K. Rakha, H. Beladi, X.Y. Xiong, and P.D. Hodgson: *J. Appl. Cryst.*, 2016, vol. 49, pp. 399–414.
25. T. Hilditch, H. Beladi, P.D. Hodgson, and N. Stanford: *Mater. Sci. Eng. A*, 2012, vol. 534, pp. 288–96.
26. ASTM E975-13: *Standard Practice for X-ray Determination of Retained Austenite in Steel with Near Random Crystallographic Orientation*, ASTM International, United States, 2013.
27. A.K. De, J.G. Speer, D.K. Matlock, D.C. Murdock, M.C. Mataya, and R.J. Comstock, Jr.: *Metall. Mater. Trans. A*, 2006, vol. 37A, pp. 1875–86.
28. B.D. Cullity and J.W. Weymouth: *Am. J. Phys.*, 1957, vol. 25, pp. 394–95.
29. N.H. Van Dijk, A.M. Butt, L. Zhao, J. Sietsma, S.E. Offerman, J.P. Wright, and S. Van der Zwaag: *Acta Mater.*, 2005, vol. 53, pp. 5439–47.
30. J.H. Hollomon: *Trans. AIME*, 1945, vol. 162, pp. 268–90.
31. D.A. Korzekwa, D.K. Matlock, and G. Krauss: *Metall. Mater. Trans. A*, 1984, vol. 15A, pp. 1221–28.
32. D.P. Koistinen and R.E. Marburger: *Acta Metall.*, 1959, vol. 7, pp. 59–60.
33. Y.J. Li, P. Choi, C. Borchers, S. Westerkamp, S. Goto, D. Raabe, and R. Kirchheim: *Acta Mater.*, 2011, vol. 59, pp. 3965–77.
34. H. Kong, Q. Chao, M.H. Cai, E.J. Pavlina, B. Rolfe, P.D. Hodgson, and H. Beladi: *Mater. Sci. Eng. A*, 2017, vol. 707, pp. 538–47.
35. F.Y. Wang, Y.F. Zhu, H.H. Zhou, B.Z. Jiang, and G. Wang: *Sci. China Technol. Sci.*, 2013, vol. 56, pp. 1847–57.
36. F. HajyAkbary, J. Sietsma, G. Miyamoto, T. Furuhara, and M.J. Santofimia: *Acta Mater.*, 2016, vol. 104, pp. 72–83.
37. E.J. Seo, L. Cho, and B.C. De Cooman: *Acta Mater.*, 2016, vol. 107, pp. 354–65.
38. F.G. Caballero, C. Garcia-Mateo, M.J. Santofimia, M.K. Miller, and C.G. De Andres: *Acta Mater.*, 2009, vol. 57, pp. 8–17.
39. J. Sun, H. Yu, S. Wang, and Y. Fan: *Mater. Sci. Eng. A*, 2014, vol. 596, pp. 89–97.
40. C. Song, H. Yu, L. Li, T. Zhou, J. Lu, and X. Liu: *Mater. Sci. Eng. A*, 2016, vol. 670, pp. 326–34.
41. J. Zhang, H. Ding, and R.D.K. Misra: *Mater. Sci. Eng. A*, 2015, vol. 636, pp. 53–59.
42. L. Cho, E.J. Seo, and B.C. De Cooman: *Scripta Mater.*, 2016, vol. 123, pp. 69–72.
43. H.K.D.H. Bhadeshia: *Metal Sci.*, 1982, vol. 16, pp. 159–66.
44. F.G. Caballero, M.J. Santofimia, C. Capdevila, C. García-Mateo, and C. García de Andrés: *ISIJ Int.*, 2006, vol. 46, pp. 1479–88.
45. M. Peet, H.K.D.H. Bhadeshia: http://www.msm.cam.ac.uk/map/steel/programs/mucg83.html. Accessed 2 May 2014.
46. H.K.D.H. Bhadeshia, I.O. Materials: Bainite in steels, *Inst. of Metals*, 1992.
47. H.K.D.H. Bhadeshia and D.V. Edmonds: *Acta Metall.*, 1980, vol. 28, pp. 1265–73.
48. X.C. Xiong, B. Chen, M.X. Huang, J.F. Wang, and L. Wang: *Scripta Mater.*, 2013, vol. 68, pp. 321–24.
49. F.G. Caballero, M.K. Miller, A.J. Clarke, and C. Garcia-Mateo: *Scripta Mater.*, 2010, vol. 63, pp. 442–45.
50. J. Sun and H. Yu: *Mater. Sci. Eng. A*, 2013, vol. 586, pp. 100–07.
51. X.-D. Tan, Y.-B. Xu, D. Ponge, X.-L. Yang, Z.-P. Hu, F. Peng, X.-W. Ju, D. Wu, and D. Raabe: *Mater. Sci. Eng. A*, 2016, vol. 656, pp. 200–15.
52. H. Rastegari, A. Kermanpur, and A. Najafizadeh: *Mater. Sci. Eng. A*, 2015, vol. 632, pp. 103–09.
53. Q. Li, X. Huang, and W. Huang: *Mater. Sci. Eng. A*, 2016, vol. 662, pp. 129–35.
54. C.H. Young and H.K.D.H. Bhadeshia: *Mater. Sci. Technol.*, 1994, vol. 10, pp. 209–14.
55. J. Shi, X. Sun, M. Wang, W. Hui, H. Dong, and W. Cao: *Scripta Mater.*, 2010, vol. 63, pp. 815–18.
56. S. Zhang and K.O. Findley: *Acta Mater.*, 2013, vol. 61, pp. 1895–1903.
57. A.S. Podder, I. Lonardelli, A. Molinari, and H.K.D.H. Bhadeshia: *Proc. R. Soc. A*, 2011, vol. 467, pp. 3141–56.
58. I.B. Timokhina, P.D. Hodgson, and E.V. Pereloma: *Metall. Mater. Trans. A*, 2004, vol. 35A, pp. 2331–41.